# X-ray computed tomography of multiple-layered scaffolds with controlled gradient cell lattice structures fabricated via additive manufacturing

**D Khrapov[1], M Surmeneva[1], A Koptioug[2], S Evsevleev[3], F Léonard[3], G Bruno[3], R Surmenev[1*]**

[1]Research School of Chemistry & Applied Biomedical Sciences, *National Research Tomsk Polytechnic University*, 30 Lenina avenue, Tomsk 634050, Russia
[2]*Mid Sweden University*, Akademigatan 1, Östersund SE-831 25, Sweden
[3]*Federal Institute for Materials Research and Testing (BAM),* Unter den Eichen 87, Berlin 12205, Germany

*E-mail: rsurmenev@mail.ru

**Abstract.** In this paper we report on the characterization by X-ray computed tomography of calcium phosphate (CaP) and polycaprolactone (PCL) coatings on Ti-6Al-4V alloy scaffolds used as a material for medical implants. The cylindrical scaffold has greater porosity of the inner part than the external part, thus, mimicking trabecular and cortical bone, respectively. The prismatic scaffolds have uniform porosity. Surface of the scaffolds was modified with calcium phosphate (CaP) and polycaprolactone (PCL) by dip-coating to improve biocompatibility and mechanical properties. Computed tomography performed with X-ray and synchrotron radiation revealed the defects of structure and morphology of CaP and PCL coatings showing small platelet-like and spider-web-like structures, respectively.

## 1. Introduction

3D scaffolds are biomaterials with predetermined architecture and optimized functionality used as implants for segmental bone reconstruction. Electron beam melting (EBM) additive manufacturing allows forming complex components from powdered precursor material by sequentially and selectively melting layers using CAD models and embedded software to control the electron beam. Although conventional micro-lining or sintering technologies do not give open cell structures from several metals or alloys (such as Ti-6Al-4V), EBM may be used to fabricate complex structures for any pre-alloyed precursor powder.

A particularly new application of EBM involves the manufacture of open cellular structures with a predetermined modulus of elasticity or stiffness ($E$). Typical example of such structures are orthopedic implants designed to prevent bone shielding (stress shielding) by reducing $E$ for high modulus solid metals by more than an order of magnitude [1-3]. Five types of scaffolds with gradient porosity based on Ti-6Al-4V-alloy with different designs and densities were manufactured and investigated by uniaxial compression tests to reveal the influence of the apparent scaffold density on mechanical properties [4]. The idea of multilayered scaffold was in mimicking different type of bone structures including cortical-like (with high density), and trabecular-like (with low density) in one scaffold. The stress-strain curves for all of samples demonstrated considerable ductility which means that parts with different porosities of multilayer scaffolds could change elastic modulus and ultimate compress

strength of the structure. Thus, gradient cellular structures manufactured by EBM from Ti-6Al-4V have certain advantageous properties for biomedical applications such as high plastic deformation and high strength [4, 5]. Biocompatibility of implants is of great importance from biomedical applications viewpoint. Therefore, our project focuses on combining complex scaffold geometries and biocompatible coatings to improve both mechanical behavior and biocompatibility of the implants for bone surgery. The aim of the study is investigating the dip-coating process of complex cellular structures and the properties of resulting coating layers by X-ray computed tomography. Issues of specific interest were the influence of scaffold geometry on the results of coating, defects of the structure itself and coating, and structure and properties of the coating. is a technique of choice to investigate these essential aspects.

## 2. Materials and methods

*2.1. Specimens*

Porous scaffolds of Ti-6Al-4V alloy were fabricated by EBM system (Arcam EBM, Mölndal, Sweden). The structures were built layer-by-layer using a precursor Ti-6Al-4V powder (Arcam AB, Mölndal, Sweden), with particle size distribution of 75-125 μm. The additive manufacturing equipment was described in [6, 7].

We fabricated porous scaffolds with two different outlines: a cylinder with an overall height of 30 mm and a diameter of 15 mm (figure 1) with a central full-length bore hole of 5 mm in diameter. The cylinder consisted of 2 coaxial zones of different density. The outer zone had a more dense structure to imitate cortical bone, whereas the inner zone with an outer diameter of 11 mm had a less dense structure to imitate trabecular bone. Outer and inner zones had diamond-like unit cell structure widely used in additive manufacturing of porous and graded lattice structures [8]. The second type of scaffold represents a prismatic structure with a height of 20 mm and a base of 10 x 10 $mm^2$ with body centered cubic (BCC) elemental cells.

We coated the fabricated scaffolds with calcium phosphate (CaP) and polycaprolactone (PCL). CaP is known for its biocompatibility and is widely used as coating for titanium and titanium alloy implants due to various surface treatments which may ensure good mechanical properties [9]. PCL is also known as an established material for bone implants, due to its biocompatibility, mechanical strength and biodegradability [10, 11] which was suggested to improve mechanical properties of the metal scaffolds.

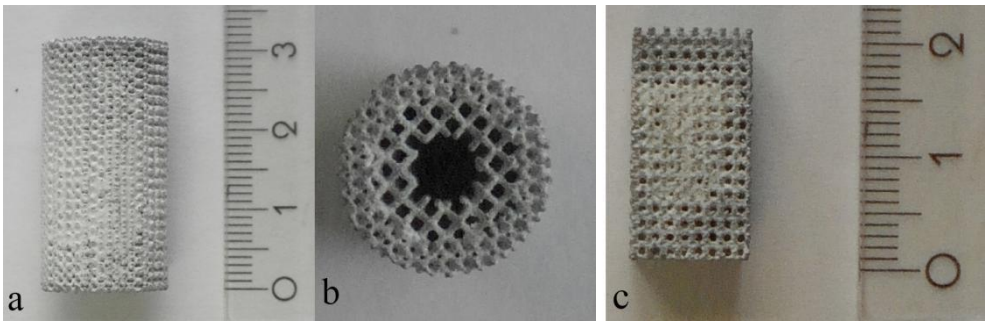


**Figure 1.** CaP coated scaffolds: a – two- zone cylindrical scaffold (side view), b – two-zone cylindrical scaffold (top view) and c – prismatic scaffold.

Modification of the scaffolds' surface with CaP was performed by dip coating method [12]. The scaffolds were dipped five times in aqueous solutions of $CaCl_2$ and NaH2PO4 diluted in distilled water with concentrations of 0,055 and 0,107 g/ml, respectively. Each dip cycle consists of two immersions in each solution sequentially for 1 minute with intermediate rinsing in distilled water.

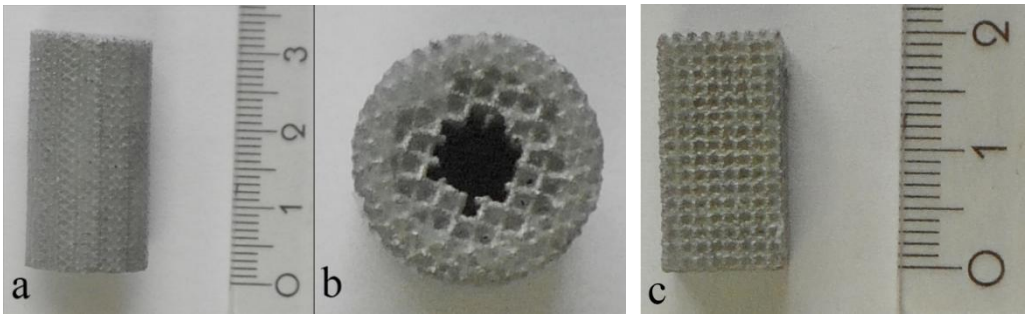


**Figure 2.** PCL coated scaffolds: a – 2 zone cylindrical scaffold (side view), b – 2 zone cylindrical scaffold (top view), c –prismatic scaffold

After 5 dip cycles pores of the scaffolds were not completely filled, indicating the imperfection of the deposition process. Therefore, scaffolds were dipped with eight more cycles in solutions of $CaCl_2$ and $NaH_2PO_4$ with the same concentrations diluted in distilled water with 25% ethanol under sonication to improve the coating process [12].

The PCL coating of the scaffolds was performed by manual dip-coating method according to a slightly changed process described in [13]. We prepared 5% PCL solution in chloroform under continuous shaking. The samples were soaked in the solution for 5 minutes prior to drying at room temperature (figure 2). The PCL was supposed to fill the inner volume of scaffolds with porosity of more than 50 % and bond struts together.

*2.2. X-ray computed tomography*

X-ray computed tomography (CT) was used to get 3D images showing internal structure of coated scaffolds. High resolution of the method allows for studying shapes of individual pores, surface roughness and structure of the coating, distribution of defects, presence of unmolten or partially-fused powder particles on the metal of scaffolds, thermal cracks [3, 14]. The CT measurements were carried out using a V|tome|x L 180/300 system from General Electrics. A voxel size of 10μm was achieved using an X-ray tube voltage of 135 kV and current of 70 μA Additionally, high resolution synchrotron CT (SRCT) was conducted on the beamline BAMline at the synchrotron BESSYII, Helmholz Zentrum Berlin. The energy of monochromatic X-ray beam was set to 50 kV and a voxel size of 0.438μm was achieved using a CCD camera with a 10x objective.

The reconstruction of 3D volumes from 2D projections of synchrotron radiation computed tomography (SRCT) data was made by BAM in-house developed filtered back projection software, and a single-distance phase-contrast correction algorithm [15], using ANKA phase software [16]. The proprietary reconstruction software from General Electric was employed for the image reconstruction in X-ray computed tomography. The reconstructed data were processed using FiJi ImageJ software and AvizoFire version 8.4 was used for 3D rendering [17].

The fine structure and small X-ray attenuation coefficient of the CaP makes it poorly distinguishable in the reconstructed volume obtained by X-ray CT (voxel size = 10 μm). Therefore, further investigation of the samples coated with CaP was performed only by synchrotron- based CT. The field of view for the setup with maximum magnification (*i.e.* pixel size of 0.438μm) available at the BAMline is 1.7mm. Since the sample dimensions exceed this value, the "region of interest SRCT" approach should be employed. In this case only a limited volume at the center of the sample can be observed limiting its application to the prismatic samples as the cylindrical ones have the central hole Therefore, the SRCT was carried out only on prismatic samples also having a shorter distance between struts (more material of interest in the field of view). Prior to analysis the reconstructed data were treated in order to correct ring artefacts and suppress noise. This allowed enhancing the contrast and improving the threshold segmentation of the Ti-6Al-4V scaffold and CaP particles.

## 3. Results and discussion

Analysis of the acquitted data reveals that CaP-based layer consists of randomly oriented platelets with CaP particles attached to the scaffold surface and filling the entire space inside one cell of the scaffold structure (figure 3a). Since the imaged region of interest is in the center of sample it is possible to suppose that CaP could fully fill the inner parts of the lattice structure after certain number of dip-coating cycles.

Figure 3b shows the surface of the Ti6Al4V scaffold itself with partially molten powder particles attached to the surface. These particles increase the surface roughness, and one can clearly see geometrical deviation of the real scaffold from the CAD model with cylindrical struts

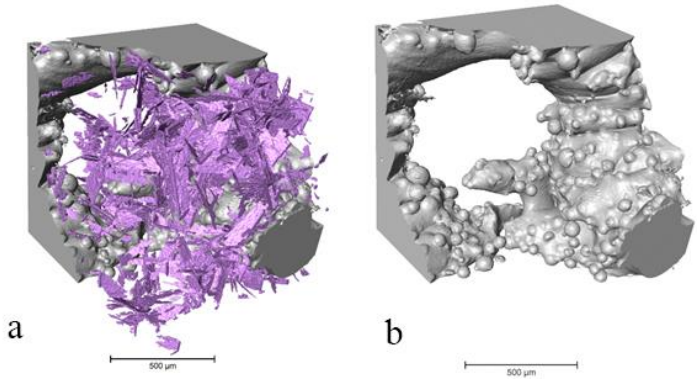


**Figure 3.** Segmented SRCT data from a prismatic structured scaffold coated with CaP: a – CaP-based platelets (in purple) and Ti-6Al-4V metallic scaffold (in grey), and b – Ti-6Al-4V metallic scaffold (in grey) with CaP digitally removed.

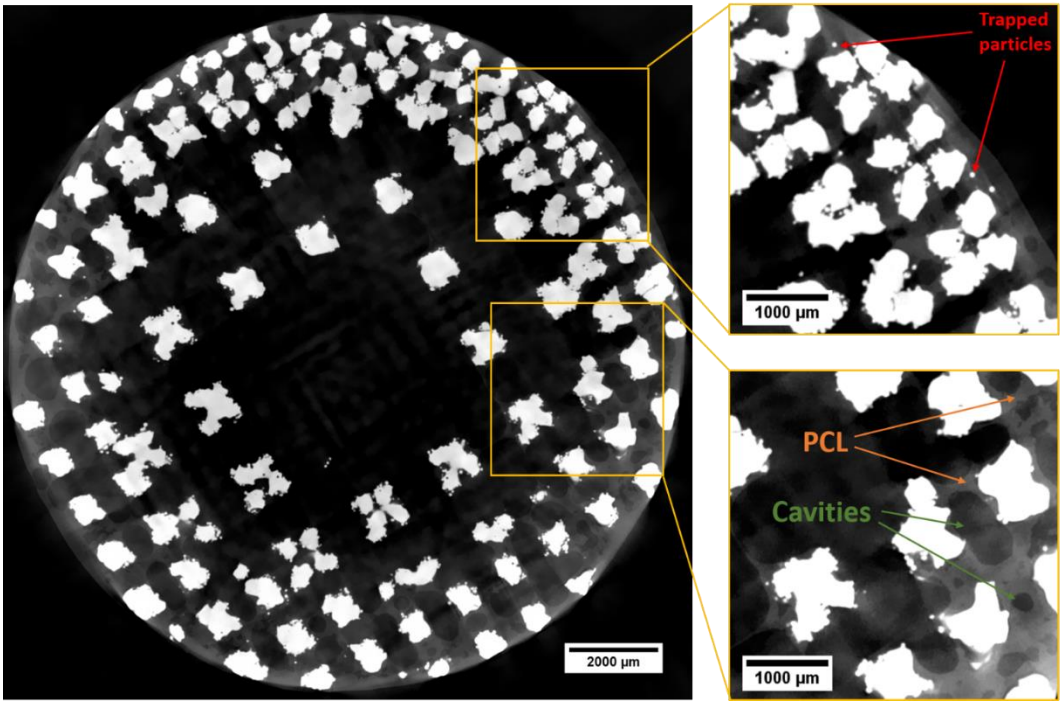


**Figure 4.** Reconstructed lab CT slice of the cylindrical sample with PCL coating: the white areas corresponds to metal (Ti-6Al-4V), the light grey color ones- to PCL, the dark grey and black ones- to air (*e.g.* cavities inside PCL).

The reconstructed slice of the cylindrical lattice sample coated with PCL is shown in figure 4. Areas with different grey level intensity correspond to different materials. Although two zone

cylindrical scaffold was completely immersed in the polymer, cavities in the dried up PCL structure were observed (figure 4). The less dense inner zone of the scaffold with larger spacing between struts is not filled by PCL, and only polymer "filaments" of 0.6-0.8 mm between the neighboring struts are observed.

Another feature that was revealed for the PCL coated samples was the presence of unattached metal powder particles inside PCL (figure 5, red color). They are mostly located in the outer sample zone with smaller spacing between struts. Most probably these are the particles left after the incomplete lattice scaffold sample cleaning after manufacturing. Thanks to PCL metal particles will not get inside the human body after implantation until PCL degrade. However, the presence of the particles indicates that a better cleaning process of the scaffolds is required after manufacturing.

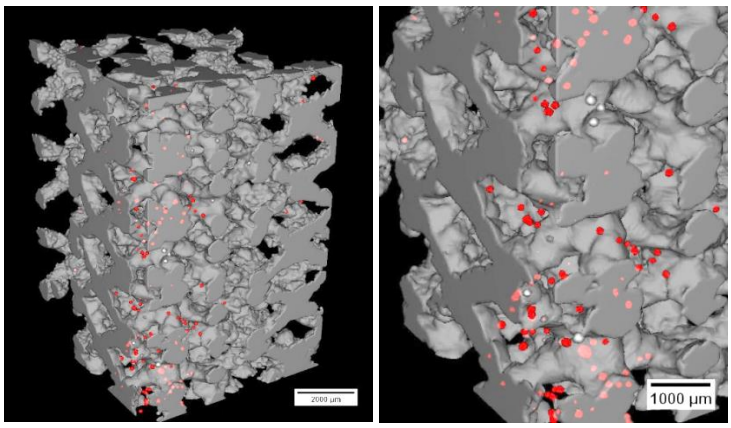


**Figure 5.** Segmented SRCT data from a part of the cylindrical sample. Red color corresponds to unattached metal powder particles trapped in the PCL.

The SRCT data showed the existence of cavities in the structure of dried PCL in the prismatic scaffold samples (figure 6), similar to the observation for the cylindrical specimen (figure 4). In addition, the attachment of PCL to the scaffold does not take place over the whole surface. Thus, a gap is formed between metal and PCL both near the latttice nodes (figure 6b) and around the lattice struts (figure 6a). Gap or void implies a lack of adhesion between metallic scaffold and polymer in some areas. This fact can be caused by pour wettability of additively manufactured Ti-Al6-V4 surfaces, presence of unwanted impuritues or by some imperfections of the coating process.

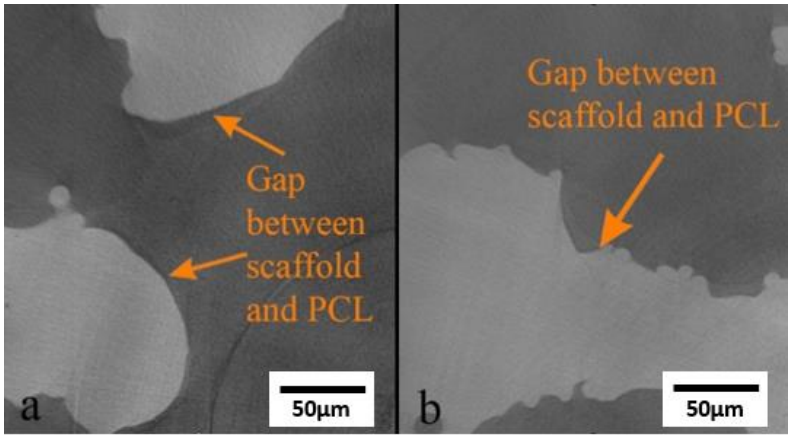


**Figure 6.** The part of reconstructed SRCT images of prismatic scaffold samples coated with PCL:a – "web-like structure" of PCL between two struts, b – PCL on the surface of the strut.

## 4. Conclusion

The dip-coating method was used to form CaP and PCL coatings on the surface of porous scaffolds prepared by electron-beam melting. With the chosen procedures CaP and PCL coatings did not completely fill the internal structure of the scaffolds, which was clearly revealed by using X-ray CT. This indicates that the process of coating needs to be modified. It is possible to suppose that CaP could fully fill the inner structure if certain number of dip-coating cycles would be conducted.

Synchrotron based computed tomography having better spatial resolution revealed the formation of cavities inside the PCL. Moreover, PCL forms "filaments" and web-like structures between neighboring struts of the scaffold, which in some cases are not fully adhered to the scaffold surface. Gaps between the polymer coatings and metal surfaces were also detected. This may be caused by imperfections of the coating process, and, possibly, by inadequate wettability of the additively manufactured Ti6Al4V surfaces. Powder particles of the precursor metal not attached to the scaffold surface spread inside PCL were observed. It indicated deficiencies in the process of scaffold cleaning after the EBM manufacturing. Nevertheless, PCL can bind the unattached particles preventing their contact with the tissue and their release from the scaffold structure.

Overall, computed tomography is a powerful non-destructive tool that can give 3D morphology of the coatings and their defects, in addition to the geometry of the scaffolds.

Future work will focus on the improvements to the coating process, and on extending the coating characterization (overall thickness, local thickness, defects size and location) and on correlating this information with the mechanical properties.

## Acknowledgments

The work was supported by Russian Science Foundation (No. 15-13-00043). The authors would like to express their gratitude to Tatiana Mishurova, Tobias Thiede, Dr Christian Gollwitzer, Dr Itziar Serrano-Munoz. The work at BAM was supported by the German-Russian Interdisciplinary Science Center (G-RISC) funded by the German Federal Foreign Office via the German Academic Exchange Service (DAAD) (Funding Decision No. T-2017b-3).

## References

[1] Murr L, Gaytan S, Medina F, Lopez H, Martinez E, Machado B, Hernandez D, Martinez L, Lopez M, Wicker R and Bracke J 2010 Next-generation biomedical implants using additive manufacturing of complex, cellular and functional mesh arrays *Phil. Trans. Roy. Soc. A.* **368** 1999

[2] Murr L, Gaytan S, Ramirez D, Martinez E, Hernandez J, Amato K, Shindo P, Medina F and Wicker B 2012 Metal fabrication by additive manufacturing using laser and electron beam melting technologies *J. Mater. Sci. Technol.* **28 (1)** 1

[3] Niinomi M 2008 Metallic biomaterials. *J. Artif. Organs.* **11** 105

[4] Chudinova E, Surmeneva M, Koptioug A, Scoglund P and Surmenev R 2016 Additive manufactured Ti-6Al-4V scaffolds with the RF-magnetron sputter deposited hydroxyapatite coating *J. Phys. Conf. Ser.* **669** 012004

[5] Surmeneva M, Surmenev R, Chudinova E, Koptioug A, Tkachev M, Gorodzha S and Rännar L 2017 Fabrication of multiple-layered gradient cellular metal scaffold via electron beam melting for segmental bone reconstruction *Mater. Des.* **133** 195

[6] Sousa I, Mendes A and Bártolo P J 2013 PCL scaffolds with collagen bioactivator for applications in Tissue Engineering. *Procedia Engineer.* **59** 279

[7] Surmeneva M, Surmenev R, Nikonova Y, Selezneva I, Ivanova A, Putlyaev V, Prymak O and Epple M 2014 Fabrication, ultra-structure characterization and in vitro studies of RF magnetron sputter deposited nano-hydroxyapatite thin films for biomedical applications *Appl. Surf. Sci.* **317** 172

[8] Elias C N, Lima J H C, Valiev R and Meyers MA 2008 Biomedical applications of titanium and its alloys *Jom.* **60** (3) 46

[9] Dinda G, Shin J and Mazumder J 2009 Pulsed laser deposition of hydroxyapatite thin films on Ti-6Al-4V: effect of heat treatment on structure and properties *Acta Biomater.* **5 (5)** pp 1821-30

[10] Cipitria A, Reichert J, Epari D, Saifzadeh S, Berner A, Schell H, Mehta M, Schuetz M, Duda G and Hutmacher D 2013 Polycaprolactone scaffold and reduced rhBMP-7 dose for the regeneration of critical-sized defects in sheep tibiae *Biomaterials* **34** 9960

[11] Dumas M, Terriault P and Brailovski V 2017 Modelling and characterization of a porosity graded lattice structure for additively manufactured biomaterials. *Materials & Design* **121**, 383

[12] Watanabe J and Akashi M 2007 Formation of hydroxyapatite provides a tunable protein reservoir within porous polyester membranes by an improved soaking process formation of hydroxyapatite provides a tunable protein reservoir within porous polyester membranes by an improved soaking process *Biomacromol.* **8 (7)** 2288

[13] Grau M, Matena J, Teske M, Petersen S, Aliuos P, Roland L, Grabow N, Escobar H, Gellrich NC, Haferkamp H and Nolte I. 2017 In vitro evaluation of PCL and P(3HB) as coating materials for selective laser melted porous titanium implants *Mater (Basel),* **10(12),** 1344

[14] Hernández-Nava E, Smith C J, Derguti F, Tammas-Williams S, Leonard F, Withers P J, Todd I and Goodall R 2016 The effect of defects on the mechanical response of Ti-6Al-4V cubic lattice structures fabricated by electron beam melting *Acta Mat.* **108** 279

[15] Paganin D, Mayo S, Gureyev T, Miller P and Wilkins S 2002 Simultaneous phase and amplitude extraction from a single defocused image of a homogeneous object *J. Microsc-Oxford* **206** 33

[16] Weitkamp T, Haas D, Wegrzynek D and Rack A 2011 ANKA phase: software for single-distance phase retrieval from inline X-ray phase-contrast radiographs *J. Synchrotron. Radiat.* **18** 617

[17] Kruth J, Bartscher M, Carmignato S, Schmitt R, De Chiffre L and Weckenmann A 2011 Computed tomography for dimensional metrology *CIRP Annals - Manufacturing Technology* **60** 821